Folate-Targeted Nanoparticles Show Efficacy in the Treatment of Inflammatory Arthritis

Thommey P. Thomas, Sascha N. Goonewardena, Istvan J. Majoros, Alina Kotlyar, Zhengyi Cao, Pascale R. Leroueil, and James R. Baker, Jr.

Objective. To investigate the uptake of a poly(amidoamine) dendrimer (generation 5 [G5]) nanoparticle covalently conjugated to polyvalent folic acid (FA) as the targeting ligand into macrophages, and to investigate the activity of an FA- and methotrexate (MTX)–conjugated dendrimer (G5-FA-MTX) as a therapeutic for the inflammatory disease of arthritis.

Methods. In vitro studies were performed in macrophage cell lines and in isolated mouse macrophages to check the cellular uptake of fluorescence-tagged G5-FA nanoparticles, using flow cytometry and confocal microscopy. In vivo studies were conducted in a rat model of collagen-induced arthritis to evaluate the therapeutic potential of G5-FA-MTX.

Results. Folate-targeted dendrimer bound and internalized in a receptor-specific manner into both folate receptor β–expressing macrophage cell lines and primary mouse macrophages. The conjugate G5-FA-MTX acted as a potent antiinflammatory agent and reduced arthritis-induced parameters of inflammation such as ankle swelling, paw volume, cartilage damage, bone resorption, and body weight decrease.

Conclusion. The use of folate-targeted nanoparticles to specifically target MTX into macrophages may provide an effective clinical approach for antiinflammatory therapy in rheumatoid arthritis.

Thommey P. Thomas, MS, PhD, Sascha N. Goonewardena, MD, Istvan J. Majoros, PhD, Alina Kotlyar, MS, Zhengyi Cao, MD, Pascale R. Leroueil, PhD, James R. Baker, Jr., MD: University of Michigan, Ann Arbor.

Address correspondence to James R. Baker, Jr., MD, Michigan Nanotechnology Institute for Medicine and Biological Sciences, Department of Internal Medicine, Division of Allergy, 1150 West Medical Center Drive, Room 9220C MSRB III, University of Michigan, Ann Arbor, MI 48109. E-mail: jbakerjr@umich.edu.

Folate receptors (FRs) comprise a family of glycosyl phosphatidylinositol–anchored, high-affinity receptors for folic acid (FA) and are the products of at least 4 different genes: FRα, FRβ, FRγ, and FRδ (1,2). Although much research has focused on folate receptor α (FRα) as a target for therapy and imaging in oncology, several recent studies have used FRβ as a therapeutic target on macrophages in inflammatory diseases (3–5). In rheumatoid arthritis (RA), for example, FRβ has been shown to be specifically expressed on activated macrophages in inflamed joints, thus providing a target for the delivery of both therapeutics and imaging agents (6–9). Studies have demonstrated the specific internalization/accumulation of radionuclide-conjugated FA in inflamed joints of mice, rats, dogs, horses, and even humans (3).

The feasibility of using FRβ to mediate the specific delivery of molecules is based on several unique biologic characteristics of the FR. First, expression of FRβ is specific to the myelomonocytic/macrophage lineages of hematopoietic cells, while there is negligible expression of this molecule on other blood cells such as lymphocytes, granulocytes, or erythrocytes (9,10). Second, elevated levels of functional glycosylated FRβ are expressed only on activated macrophages involved in inflammatory responses, but not on quiescent resident macrophages (5,11). In addition, FRα is known to be preferentially expressed at the apical (luminal) side (e.g., the urine side in kidney tubules and the air sac side of the lungs) of normal tissues; therefore, it is possible that there will be minimal FRα binding of circulating folate-targeted drugs in normal tissues (12). Finally, although free FA and methotrexate (MTX) can access normal cells through the ubiquitously expressed reduced folate carrier (RFC), uptake through this channel does not occur when FA or MTX is conjugated to a macromole-

cule like a nanoparticle. These findings together suggest that activated macrophages are the only predominant normal cells that could specifically bind and internalize folate-targeted nanoparticle drugs from circulation through FRβ.

MTX is an "antifolate" drug that competes with FA for binding to the dihydrofolate reductase enzyme and blocks the 1-carbon transfer reaction used in the biosynthesis of nucleotides. This inhibits DNA formation and results in reduced cell proliferation and induction of apoptosis. For more than 2 decades MTX has been employed as a disease-modifying antirheumatic drug (DMARD) for the treatment of RA, either as a single agent or in combination with biologics such as tumor necrosis factor (TNF) inhibitors (13,14). The mechanisms by which MTX suppresses arthritis are complex and may extend beyond the inhibition of DNA synthesis in inflammatory cells. These mechanisms may include increased release of adenosine, altered production of cytokines, formation of reactive oxygen species, T cell apoptosis, and suppression of B cell responses (4,15,16). Several studies have suggested that at least one mechanism for MTX activity in RA is through antiproliferative effects on activated macrophages following specific uptake into these cells via FRβ (4,5,9,10,13,15,17–19). Unfortunately, approximately one-third of RA patients respond poorly to MTX, while another one-third develop toxic side effects. Patients with increased side effects may have polymorphisms in proteins such as RFC and 5,10-methylenetetrahydrofolate reductase involved in the transport and metabolism of free MTX (20–22). Since the side effects of MTX are the result of its action on normal cells, either preventing the uptake of MTX in normal cells or specifically targeting MTX to inflammatory cells independent of the RFC may prevent these problems.

Poly(amidoamine) (PAMAM) dendrimers have been extensively employed as a macromolecular delivery platform and have several attractive properties for this purpose (Figure 1). These properties include uniformity, biocompatibility, defined structure, and the capability to chemically couple multiple molecular entities to primary surface amino groups (23–26). Many biologic functions of molecules coupled to the dendrimer's surface are retained with a variety of molecules including hormones such as FA (27,28), peptides (29), antibodies (30), chemotherapeutic drugs (28,31), or an apoptosis-sensing fluorochrome (32). Importantly, prior studies from our laboratory have shown that dendrimers bearing FA can target FRα-expressing xenograft tumors in mice and increase the therapeutic index of carried MTX >10-fold
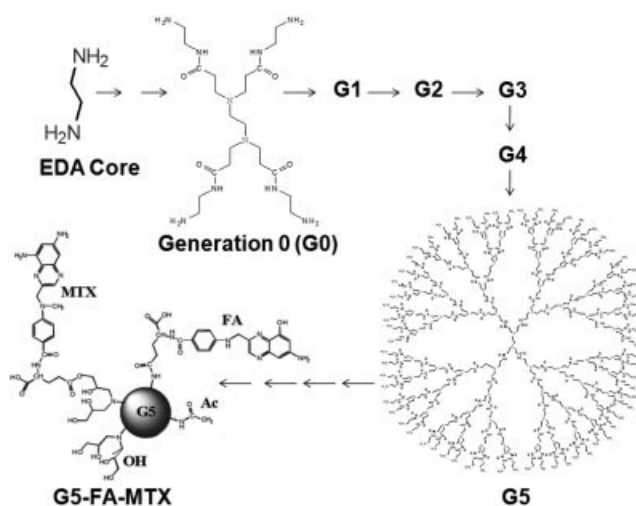

Figure 1. Schematic representation of the structures and synthesis of different generations of poly(amidoamine) dendrimers, starting from the ethylene diamine (EDA) core, and that of the functionalized dendrimer conjugate G5-FA-MTX. The details of the synthesis steps and characterization of the conjugate have been previously described (24,28). Briefly, Michael addition of methylacrylate to EDA followed by condensation reaction (amidation) yields the generation 0 (G0). These reaction steps are then repeated to obtain the higher generations as shown. The G5 is partially (60–70%) acetylated (Ac), the folic acid (FA) is incorporated through amide linkage, followed by glycidolation (to fully neutralize the surface), and finally the methotrexate (MTX) is conjugated through ester linkage.

(31). In another study, the antiinflammatory drug indomethacin encapsulated in a generation 4 (G4) dendrimer–FA conjugate has been shown to preferentially target inflamed tissues in rats, presumably by targeting FRβ in macrophages (33). In the present study, we investigated using FA-bearing G5 dendrimers to target macrophages in vitro and deliver MTX as an antiinflammatory agent in a collagen-induced arthritis model in rats.

MATERIALS AND METHODS

Materials. G5 PAMAM was synthesized and characterized at the Michigan Nanotechnology Institute for Medicine and Biological Sciences, the University of Michigan, or Dendritech. Methanol (high-performance liquid chromatography [HPLC] grade), acetic anhydride (99%), triethylamine (99.5%), DMSO (99.9%), dimethylformamide (99.8%), glycidol, 1-[3-(dimethylamino)propyl]-3-ethylcarbodiimide HCl (98%), citric acid (99.5%), sodium azide (99.99%), and D_2O were from Sigma. Fluorescein isothiocyanate (FITC) and 5-TAMRA (5T), succinimidyl ester were purchased from Invitrogen. The murine macrophage cell lines RAW 264.7 and J774 were obtained from American Type Culture Collection. The low–FR expressing MCA-207 mouse sarcoma cell line was kindly provided by Dr. Kevin McDonough at the University of

Table 1. Physical properties of the different conjugates in the study*

	Hydrodynamic diameter, nM†	Poly dispersity index‡	Zeta potential§	Purity, %¶	Average molecular weight, kd#	Average number of FA molecules per dendrimer**	Average number of MTX molecules per dendrimer**	Average number of 5-TAMRA molecules per dendrimer	Average number of FITC molecules per dendrimer
G5-FITC	5.6	1.012	–	>98	34.4	–	–	–	4.6
G5-FITC-FA-1	5.9	1.058	–	>98	40.5	4.3	–	–	5.2
G5-FITC-FA-2	–	–	–	>95	38.3	4.0	–	–	3.0
G5-5T	6.0	1.017	–	>99	34.1	–	–	6.2	–
G5-5T-FA	7.6	1.092	–	>99	35.8	4.1	–	5.3	–
G5-FA-MTX-1	5.9	1.125	11.9	>99	40.7	2.5	8.0	–	–
G5-FA-MTX-2	6.1	1.096	7.4	>99	38.2	5.0	10.5	–	–

* The analytic data shown were obtained at the Michigan Nanotechnology Institute for Medicine and Biological Sciences (for G5-FITC, G5-FITC-FA, G5-5T, and G5-5T-FA); at the National Characterization Laboratory, National Cancer Institute (for drug conjugates); and at Cambrex (the number of ligands for G5-FA-MTX-2). FA = folic acid; MTX = methotrexate; FITC = fluorescein isothiocyanate; G5 = generation 5; 5T = 5-TAMRA.
† Calculated as the volume-weighted average over a particular range of size populations corresponding to the most prominent peak in the percent volume distribution obtained in dynamic light scattering.
‡ A measure of the distribution of molecular mass, with a value of 1 for a fully homogeneous population of molecules.
§ An index of the charge on the dendrimer, measured in phosphate buffered saline. The mean ± SD zeta potential of the amine-terminated starting dendrimer was 58.4 ± 1.3. The slightly positive zeta potential for the conjugate may be attributed to residual secondary amines on the surface.
¶ Based on high-performance liquid chromatography analysis of percent conjugate peak area versus total peak areas.
# Determined by size-exclusion chromatography coupled with multiple-angle laser light scattering and by matrix-assisted laser desorption ionization–time-of-flight mass spectrometry analyses.
** Determined by ultraviolet-visible spectroscopy and gel-permeation chromatography–multiple-angle laser light scattering.

Kentucky, Louisville. The RPMI 1640 cell culture medium, trypsin-EDTA, penicillin/streptomycin, Dulbecco's phosphate buffered saline (PBS; pH 7.4), Hanks' balanced salt solution (HBSS), and fetal bovine serum (FBS) were from Gibco BRL. Brewer Thioglycollate Medium was prepared by suspending 4.05 grams of Brewer Thioglycollate Medium Powder (Sigma) in 100 ml deionized water, boiling to dissolve the medium completely, and autoclaving at 15 lbs/in^2 pressure (at 121°C) for 15 minutes.

Synthesis and characterization of the dendrimer conjugates. The intermediates of the synthesis were extensively purified by dialysis and/or ultrafiltration before proceeding to the subsequent synthetic step. The final products and all intermediates have been characterized using ^{1}H nuclear magnetic resonance (^{1}H-NMR), matrix-assisted laser desorption ionization–time-of-flight mass spectrometry, HPLC, gel-permeation chromatography, and ultraviolet spectroscopy, as we have described previously (28,32,34). A summary of the synthetic procedures used is given below, and the physical properties of the different conjugates are given in Table 1.

FITC conjugates. The FITC conjugates G5-acetyl(Ac)(74)-FITC(5)-Gly(31) (G5-FITC) and G5-Ac(74)-FITC(5)-FA(4)-Gly(26) (G5-FITC-FA-1) were synthesized and characterized using methods previously described (the numbers of each ligand present per conjugate molecule are given in parentheses) (28). G5-FITC(3)-FA(4)-Gly(103) (G5-FITC-FA-2) was synthesized as described (35). The molecular weight of the material was determined by gel-permeation chromatography, and the number of ligands (FA/FITC) on average attached to the dendrimer surface was calculated using this value in combination with ^{1}H-NMR, accompanied by potentiometric titration of the starting G5-NH$_2$ dendrimer (Table 1).

MTX conjugates. Two large-scale batches of G5-Ac-FA-Gly-MTX (G5-FA-MTX-1 and G5-FA-MTX-2) were synthesized and characterized by Cambrex and by the National Characterization Laboratory, National Cancer Institute, using protocols similarly described (28) (Figure 1 and Table 1).

5-TAMRA conjugates. The conjugates G5-Ac(65)-5T(5)-Gly(48) (G5-5T) and G5-Ac(65)-5T(5)-FA(4)-Gly(40) (G5-5T-FA) were synthesized and characterized using procedures similar to those described for the synthesis of 6-TAMRA–based conjugates (36) (see Supplementary Data, available on the *Arthritis & Rheumatism* Web site at http://onlinelibrary.wiley.com/journal/10.1002/(ISSN)1529-0131).

Cell culture and in vitro studies. RAW 264.7 cells were cultured at 37°C in a humidified atmosphere of 5% CO$_2$ and 95% air, in RPMI 1640 medium containing 10% FBS supplemented with penicillin (100 units/ml) and streptomycin (100 μg/ml). The 10% FBS resulted in a final FA concentration equivalent to that present in human serum (~20 nM) and is designated "low FA medium." The J774 and MCA-207 cell lines were cultured in Dulbecco's modified Eagle's medium under similar conditions. In order to induce the expression of FR, the medium was switched to FA-free RPMI 1640 with 10% FBS 5–7 days prior to performing experiments. Cells were plated in low FA medium in 24-well plates (for flow cytometry) or in 35-mm dishes with glass-chambered slides (for confocal microscopy).

Isolation of mouse peritoneal cavity macrophages. Mouse peritoneal cavity macrophages were isolated using the procedure described previously (37). Briefly, the mice were injected intraperitoneally with ~2 ml of Brewer Thioglycollate Medium 6 days prior to cell isolation. The abdominal wall was exposed, washed with 70% alcohol, and injected with ~5 ml of a solution of HBSS containing 5% FBS and 10 units/ml sodium

heparin. The peritoneal fluid formed was aspirated gently. The cells were collected by centrifugation at 300g for 10 minutes at 4°C. The cell pellet obtained was suspended in 1 ml 10% HBSS, vortexed for 10–15 seconds to lyse any red blood cells, and diluted to isotonicity with HBSS. The cells were spun, counted, and resuspended in a medium containing RPMI 1640 with 20% FBS, 15 mM HEPES, 20 mM L-glutamine, 50 μM 2-mercaptoethanol, and 50 μg/ml gentamicin, and transferred to 12-well plates, and the dishes were incubated for 1 hour at 37° in a humidified 5% CO_2 incubator to allow the macrophages to attach to the dish. The nonadherent cells were removed and rinsed to remove any residual loosely adherent cells, and were then incubated with low folate medium overnight at 37°C in a humidified 5% CO_2 incubator. The medium was changed to fresh medium prior to addition of the conjugates.

Flow cytometry studies. The binding of fluorescence-labeled FA-conjugated dendrimers (G5-FITC-FA) to macrophages (RAW 264.7 cells and mouse peritoneal cavity macrophages) was evaluated using a Beckman Coulter EPICS-XL MCL flow cytometer, and the data were analyzed using Expo32 software (Beckman Coulter). The viable cells were gated, and the mean fluorescence channel 1 (FL1) fluorescence of 10,000 cells was quantified.

Confocal microscopy studies. The RAW 264.7 macrophage cell line was visualized using an IX81 inverted microscope (Olympus America) equipped with an FV1000 confocal unit and a 60×/1.4 numerical aperture/0.15-mm oil immersion objective. For cell imaging, macrophages were plated in glass-chambered dishes (Nalge Nunc International) and allowed to adhere for 24 hours at 37°C, followed by washing 2 times with PBS to remove nonadherent cells. For in vitro staining, cells were incubated with G5-5T-FA (30 nM) at 37°C for 1 hour before washing 2 times to remove unbound dendrimer conjugate. A 543-nm HeNe laser was used to excite the dendrimer–5-TAMRA, and a 405-nm laser diode was used to excite the DAPI fluorophore. Two-color imaging was performed with 2 spectral detectors (for DAPI, excitation 405 nm, detector range 455 nm; for the dendrimer–5-TAMRA, excitation 543 nm, detector range 573–648 nm). Images were processed using FLUOVIEW software (Olympus America).

In vivo studies in a rat arthritis model. The in vivo studies were conducted at Bolder BioPATH Inc. Female Lewis rats (Charles River) weighing an average of 150 grams on day 0 of the study were acclimated to the laboratory conditions for ~7 days. The animals were anesthetized with isoflurane and given subcutaneous/intradermal injections of 300 μl of Freund's incomplete adjuvant (Difco) containing 2 mg/ml bovine type II collagen (Elastin Products) at the base of the tail and at 2 sites on the back on days 0 and 6. Drug dosing was initiated on day 0 of the study and continued through day 16. Immunized rats (n = 10 per group) were treated intravenously 3 times per week with 70 mg/kg G5-FA-MTX (G5-FA-MTX-1 or G5-FA-MTX-2; 2 separate batches, equivalent to 5 mg/kg MTX), 0.2 mg/kg free MTX, or normal saline. Control immunized rats (n = 4) were also treated with normal saline using a similar regimen. The rats were weighed on days 0, 3, 6, and 9–17 of the study, and caliper measurements of the ankles were obtained every day beginning on day 9. After a final body weight measurement on day 17, animals were euthanized, blood was drawn for serum, and tissues were collected. Hind paws were transected at the level of the medial and lateral malleolus, weighed, and placed in formalin, with knees, for microscopy. For histopathologic evaluation, preserved and decalcified (5% formic acid) ankle and knee joints were cut in half longitudinally (ankles) or in the frontal plane (knees), processed through graded alcohols and a clearing agent, infiltrated and embedded in paraffin, sectioned, stained with toluidine blue, and analyzed by microscopy.

RESULTS

In vitro studies. We initially determined the time- and dose-dependent uptake of the fluorescent conjugate G5-FITC-FA in the RAW 264.7 cells by flow cytometric analysis. We have used 2 separate lots of G5-FITC-FA in this study. Both of these lots were initially tested in KB cells (which express high levels of FR) and were shown to bind in a dose-dependent and receptor-saturable manner, and the binding was completely inhibited by 50-fold excess free FA (data not shown). An initial time-course analysis using G5-FITC-FA-1 showed that the conjugate bound to the RAW cells in a time-dependent manner with maximum binding at 3–4 hours (at 300 nM, G5-FITC-FA-1 showed a mean $\pm$ SD FL1 fluorescence of 154 $\pm$ 7 at 4 hours). As shown in Figure 2A, G5-FITC-FA-2 was taken up into the RAW 264.7 cells in a dose-dependent manner. The macrophage-activating agent lipopolysaccharide failed to show any increase in the uptake of the conjugate up to 100 nM of the conjugate, but showed a modest increase at 300 nM. The control conjugate G5-FITC (300 nM) failed to show any significant uptake into the RAW 264.7 cells up to 4 hours. (Incubation with 300 nM of G5-FITC yielded a net mean $\pm$ SD FL1 fluorescence of 5.9 $\pm$ 0.7.)

Since the autofluorescence of RAW 264.7 cells at the emission wavelength of FITC was significant for confocal analysis, we synthesized conjugates using the dye 5-TAMRA, whose excitation/emission wavelength did not result in significant autofluorescence. As shown in Figure 2B, G5-5T-FA was internalized into the RAW 264.7 cells, showing localization in the cytosolic compartment. Consistent with the flow cytometric analysis, the control conjugate G5-5T failed to show any cellular accumulation. We also tested the conjugate uptake in the mouse macrophage cell line J774 and compared it with that of the low–FR expressing mouse sarcoma cell line MCA-207 (38). In cells treated with 100 nM G5-FITC-FA-1 for 1 hour, flow cytometric analysis yielded the mean $\pm$ SD FL1 fluorescence values of 20.9 $\pm$ 8.5 and 4.7 $\pm$ 0.8 in excess of those for PBS controls for the J774 and MCA-207 cells, respectively. This is consistent with our previous studies showing lack of cytotoxicity of a G5-FA-MTX drug conjugate in the MCA-207 cells during a 3-day incubation period (38).
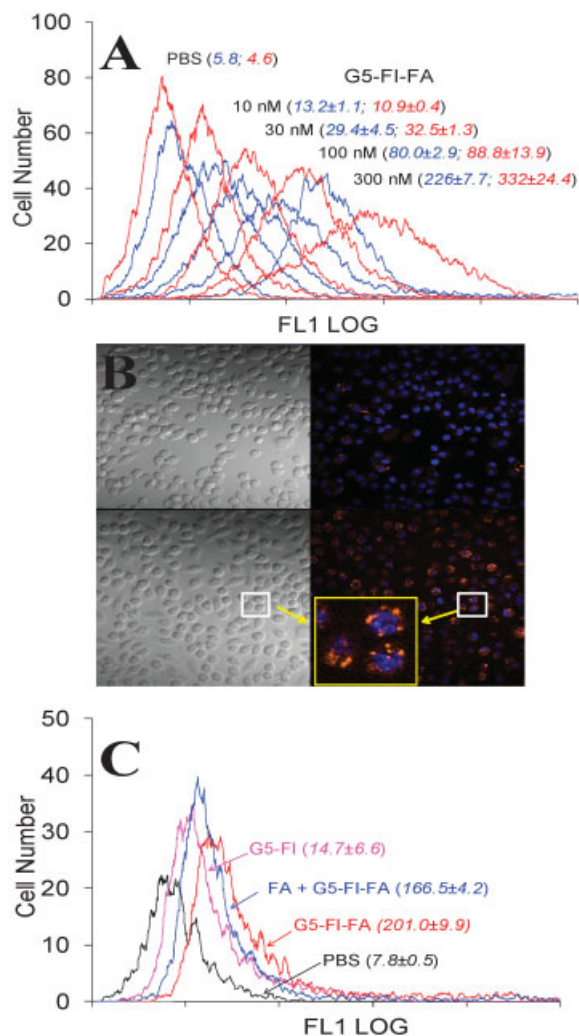
We then isolated mouse peritoneal cavity macro-

Figure 2. A, Dose-dependent binding of the fluorescein isothiocyanate (FITC) conjugate G5-FITC-FA-2 (G5-FI-FA) (at 3 hours of incubation) to RAW 264.7 cells in the presence (red) or absence (blue) of 1 μg/ml lipopolysaccharide (15 hours of preincubation), analyzed by flow cytometry. Mean ± SD fluorescence (in parentheses) under both conditions is shown. **B,** Confocal images of RAW 264.7 cells incubated with the indicated conjugates (orange) and the nuclei stained with DAPI (blue). Left panels show light microscopy. Right panels show fluorescence microscopy of the same field. The 2 small boxes are the same areas containing the 3 cells in the larger box. The larger box is at higher magnification to demonstrate the uptake of the targeted, fluorescent dendrimers in the cells. Original magnification × 60. **C,** Binding of G5-FITC-FA on isolated mouse peritoneal cavity macrophages. Mouse peritoneal cavity macrophages were incubated with 1 μM of G5-FITC (G5-FI) or G5-FITC-FA-1 (G5-FI-FA) at 37°C for 2 hours in the presence (blue) or absence (red) of 100-fold excess of free FA, and the mean ± SD fluorescence (in parentheses) was quantified. The mean ± SD fluorescence for the folate receptor–negative MCA-207 cells and the J774 macrophage cells treated with G5-FITC-FA-1 was 4.7 ± 0.8 and 20.9 ± 8.5 (at 100 nM and 1 hour of incubation), respectively, in excess of that for phosphate buffered saline (PBS) controls. The data shown are representative of treatments made in triplicate wells, with similar results obtained in an independent experiment. See Figure 1 for other definitions.

phages and tested the uptake of G5-FITC-FA conjugate in these cells. As had been observed for the cultured macrophage cell lines given above, G5-FITC-FA-1 bound to the mouse peritoneal cavity macrophages, whereas the control conjugate G5-FITC showed only low binding (Figure 2C). In order to test the FR specificity of the conjugate, we tested the effect of preincubation of cells with excess free FA. A 100-fold molar excess of free FA partially blocked the binding of G5-FITC-FA in the mouse peritoneal cavity macrophages (Figure 2C). Similar partial blocking of the uptake of G5-FITC-FA by excess free FA was also observed in the RAW 264.7 cells (data not shown).

In vivo studies in rats with collagen-induced arthritis. Our previous studies demonstrated that the dendrimer conjugate G5-FA-MTX acts as a tumoricidal agent in vivo in the KB xenograft mouse tumor model with a higher therapeutic index than free MTX (31). G5-FA-MTX for these studies was synthesized using the same multistep procedure (28) and then tested in female Lewis rats using a 17-day type II collagen–induced arthritis protocol. The rats with collagen-induced arthritis (n = 10 for each group) were treated intravenously 3 times a week with vehicle (saline), 2 different batches of G5-FA-MTX (70 mg/kg for each conjugate, equivalent to 5 mg/kg of MTX), or free MTX (0.2 mg/kg), and the nonarthritic control rats (n = 4) were similarly treated with vehicle (saline). Efficacy evaluation was based on ankle caliper measurements, animal body weight measured from day 9 to day 17, and histopathologic analysis performed on day 17 following euthanasia of the animals.

As shown in Figure 3, the increased ankle diameter and paw weight measurements caused by arthritis were decreased in rats treated with the conjugate. Significant inhibition of ankle diameter (measured by area under the curve) was seen in rats treated with G5-FA-MTX-1 (88% inhibition), G5-FA-MTX-2 (101% inhibition), or MTX (54% inhibition), as compared to disease controls. Final paw weights were significantly inhibited by treatment with G5-FA-MTX-1 (89% inhibition), G5-FA-MTX-2 (105% inhibition), or MTX (46% inhibition), as compared to disease controls. Moreover, significant inhibition of body weight loss due to arthritis was seen in rats treated with G5-FA-MTX-1 (42% inhibition), G5-FA-MTX-2 (48% inhibition), or MTX (38% inhibition), as compared to disease controls (Figure 3).

Histopathologic evaluations at the end of the study analyzing ankle and knee inflammation and pannus infiltration, cartilage damage, and bone resorption clearly indicated protection from arthritis-altered parameters by treatment with the conjugates and free MTX.
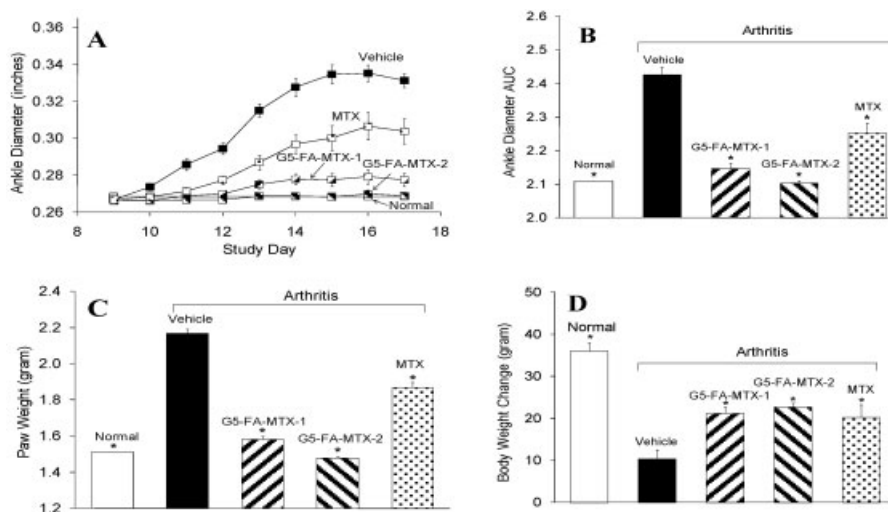
Figure 3. Effect of G5-FA-MTX treatment on ankle diameter, paw weight, and body weight of arthritic rats. **A, C,** and **D,** Normal and arthritic rats were treated with free MTX (0.6 mg/kg/week), G5-FA-MTX-1 or G5-FA-MTX-2 (225 mg/kg/week, equivalent to 15 mg/kg/week MTX), or vehicle, and the ankle diameter on days 9–17 (**A**), paw weight (**C**), and body weight on days 0–17 (**D**) were measured. **B,** Area under the curve (AUC) for the data in **A** was calculated. Values are the mean $\pm$ SD. $* = P < 0.05$ versus vehicle. See Figure 1 for other definitions.

As shown in Figure 4C, normal rats treated with vehicle showed normal synovium and normal cartilage with no pannus or bone destruction. Arthritic rats treated with vehicle had severe synovitis, moderate cartilage damage, and mild pannus and bone destruction. Arthritic rats treated with G5-FA-MTX-1 and G5-FA-MTX-2 had minimal synovitis, no cartilage damage, and no pannus or bone destruction. Arthritic rats treated with free MTX had moderate synovitis, minimal cartilage damage, and minimal pannus and bone destruction. Photomicrographs with identical trends were observed for the knee histopathology from the respective groups (not shown). These parameters were scored on a scale of 0 to 5, with 0, 1, 2, 3, 4, and 5 scored as normal, minimal, mild, moderate, marked, and severe, respectively. The effects of the drug conjugates were, however, significantly greater than those of free MTX.

We also examined the effects of the conjugates and the free MTX on organ weights of the animals (Figure 5). Relative liver and thymus weights for treatment groups did not differ significantly from those for disease controls. Relative spleen weights were significantly increased (above those for normal and disease controls) following treatment with G5-FA-MTX-1 (18% increase) or G5-FA-MTX-2 (12% increase), and were significantly reduced (below those for normal and disease controls) following treatment with MTX (9% decrease).

An independent study was conducted to test the dose-responsive efficacy of the conjugate versus that of free MTX (see Figure S1, available on the *Arthritis & Rheumatism* Web site at http://onlinelibrary.wiley.com/journal/10.1002/(ISSN)1529-0131). At the maximum dose used for the conjugate (225 mg/kg/week) and at the known maximum tolerated dose for MTX (2 mg/kg/week), the ankle diameters were reversed to the normal control values.

DISCUSSION

Several lines of evidence have indicated that macrophage activation plays a significant role in the inflammatory pathogenesis of RA (39–42). The concept of targeting macrophages through FRβ to treat RA is supported by the expression of this target in activated macrophages (39–42), the effectiveness of MTX as a drug for RA (13,14,42,43), and our previously documented utility of G5-FA-MTX as a therapeutic agent in FRα-expressing tumor models. We therefore sought to examine G5-FA-MTX as a DMARD in vivo in a collagen-induced arthritis model in rats. The results of our studies provide clear evidence that G5-FA-MTX acts as a targeted therapeutic for macrophages through FRβ effectively suppressing inflammation and arthritis in the rat model.
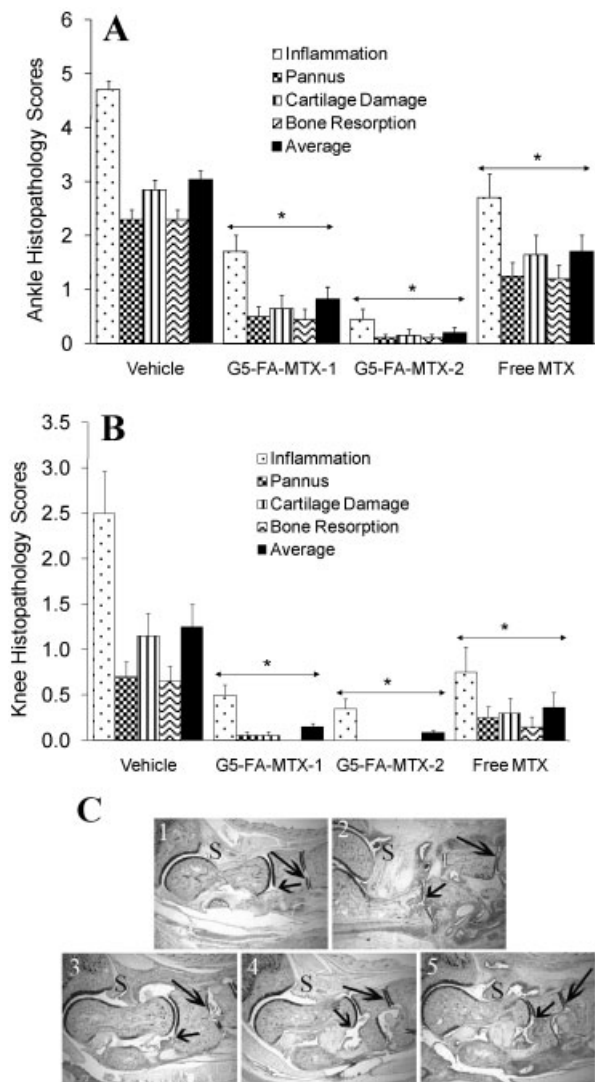
Our initial in vitro studies documented that a

Figure 4. A and **B,** Histopathologic evaluation of the ankles (**A**) and knees (**B**) of arthritic rats treated for 17 days with G5-FA-MTX or free MTX, obtained from animals in the same experiment as presented in Figure 3. Values are the mean ± SD. ∗ = $P < 0.05$ versus vehicle. For each of the indicated treatment conditions, the bars represent (from left to right) inflammation, pannus, cartilage damage, bone resorption, and the average of these 4 parameters. For control nonarthritic rats, these parameters were all scored as zero (not shown). **C,** Representative photomicrographs of stained ankle from normal rats (**1**) and from arthritic rats treated with vehicle (**2**), G5-FA-MTX-1 (**3**), G5-FA-MTX-2 (**4**), and MTX (**5**). **S** = synovium. **Arrows** indicate cartilage and pannus. Original magnification × 16. See Figure 1 for other definitions.

FITC-labeled, folate-targeted nanoparticle (G5-FITC-FA) bound to both FRβ-expressing macrophage cell lines and activated peritoneal macrophages in a receptor-specific manner, and subsequent confocal microscopic analysis demonstrated the internalization

and cytosolic localization of 5-TAMRA–labeled folate-targeted nanoparticles in RAW 264.7 cells. The receptor specificity of this binding was apparent given that the FA conjugate bound to the FR-expressing macrophages and cell lines, while control dendrimer conjugates lacking folate, G5-FITC and G5-5T, failed to bind to these cells. In contrast to our previous studies in KB cells (28), however, the binding of G5-FITC-FA could only be partially inhibited by excess free FA. The reasons for this incomplete inhibition are not clear, but given that the
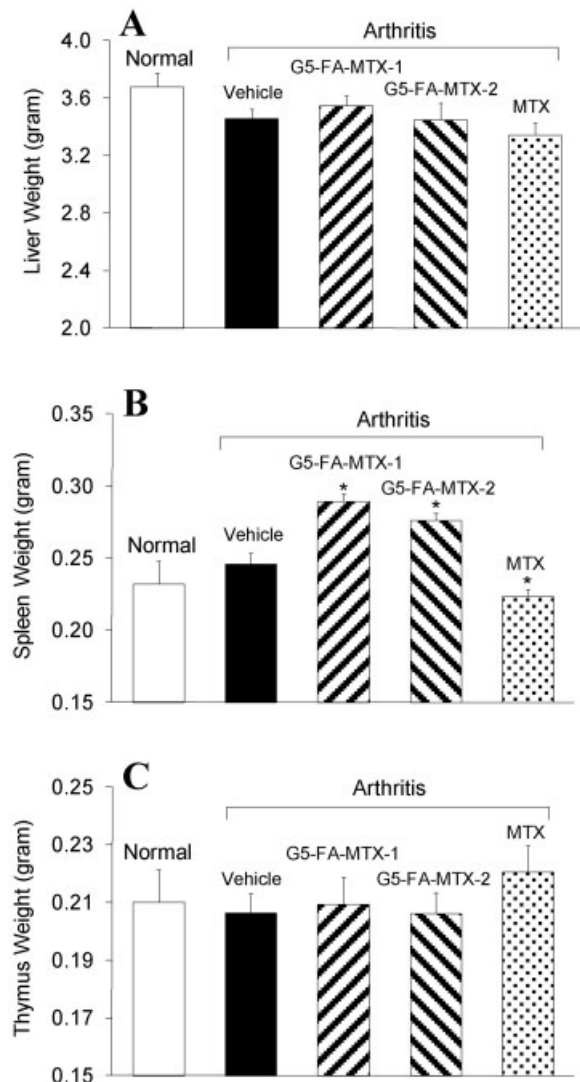

Figure 5. Effect of G5-FA-MTX on the relative weights of liver (**A**), spleen (**B**), and thymus (**C**). Rats with collagen-induced arthritis (n = 10) were treated with free MTX, G5-FA-MTX-1 or G5-FA-MTX-2, or vehicle, and the organ weights were measured on the 17th day of treatment. Values are the mean ± SD percent contributed by each organ to the body weight of the individual animals. ∗ = $P < 0.05$ versus vehicle. See Figure 1 for definitions.

control conjugates G5-FITC and G5-5T were not taken up by macrophages, it is unlikely that a portion of the uptake of the targeted conjugate was not dependent on FRβ. Our findings are similar to those of a previous study that showed that the uptake of FA-targeted liposomes was completely inhibited by free FA in FRα-expressing IGROV cells but was only ~50% inhibited by free FA in FRβ-expressing macrophages (44). While it is tempting to speculate that polyvalent binding of the FA-targeted nanoparticle to FRβ-expressing macrophages is more avid and therefore more difficult to compete with than the FRα-expressing KB cells, this finding requires more extensive examination.

Our in vivo studies in the collagen-induced rat arthritis model clearly documented that administration of G5-FA-MTX yields significant and beneficial protection from the inflammatory characteristics of collagen-induced arthritis (Figure 3). In addition, the time-dependent increase in the ankle diameter and paw weight associated with arthritis was almost completely prevented by administration of the G5-FA-MTX conjugate. Moreover, weight loss due to arthritis was prevented in rats treated with the conjugate (Figure 3), and necropsy histopathology substantiated the prevention of the inflammatory pathology of the arthritis (Figure 4). Thus, essentially all arthritis-induced effects, including infiltration of inflammatory cells, edema of the knee and ankle, pannus infiltration in cartilage and bone, cartilage damage, and bone resorption were all significantly prevented by the targeted conjugates (G5-FA-MTX-1 and G5-FA-MTX-2) (Figure 4). Importantly, as compared to animals treated with free MTX, the G5-FA-MTX conjugate–treated animals showed no abnormalities in their spleen tissue architecture (Figure 5B). This suggests high efficacy for this conjugate in treating joint inflammation, with the potential for fewer side effects.

Although the inflammatory symptoms were almost completely reversed to normal by the conjugates and MTX, the body weight loss was only partially reversed by the drugs (Figure 3). The reason for this is not clear and may be related to handling of the animals. In this regard, a similar discrepancy has been observed with Lewis rats treated with MTX and cyclosporin A (45). In addition, we used a cumulative dose of 0.6 mg/kg/week of free MTX and 15 mg/kg/week of conjugate MTX equivalent. Although the maximum tolerated dose of free MTX in Lewis rats is ~2 mg/kg/week (46), the observed lack of toxicity of the conjugates at 7.5-fold excess of the maximum tolerated dose predicts the increased therapeutic index of the targeted drug as compared to that of the free MTX. A dose-responsive efficacy study (see Figure S1, available on the *Arthritis & Rheumatism* Web site at http://onlinelibrary.wiley.com/journal/10.1002/(ISSN)1529-0131) showed that the complete reversal of the symptoms of the arthritis required that free MTX levels be at the maximum tolerated dose of MTX (~2 mg/kg/week). The conjugate showed similar maximum efficacy at ~225 mg/kg/week (equivalent to 15 mg/kg/week MTX), which is ~60% of its maximum tolerated dose. The apparent increased therapeutic index of the conjugate versus that of MTX may be attributed to the fact that the conjugate is primarily targeted to the macrophages only through FRβ, whereas the free MTX is taken up nonspecifically through the RFC, which is ubiquitous in cells. Single- and multiple-dose studies of the targeted drug in rats and dogs revealed no dose-limiting toxicity at the concentrations used in this study, also suggesting a wide therapeutic index for this compound (Laveglia, JG, PhD, MPI Research, Mattawan, MI: personal communication).

Taken together, our studies provide evidence that the in vivo effect of G5-FA-MTX is a consequence of targeted drug delivery into macrophages. This parallels our prior work that showed the specific targeting of G5-FA-MTX into FR-expressing tumor cells and the current studies documenting the inability of this conjugate to be taken up by FR-negative cells. This was reinforced by previous studies suggesting the in vitro and in vivo macrophage uptake of other FA-conjugated molecules (6–9) and the in vitro documentation of targeted uptake of G5-FITC-FA into macrophages in this work (Figure 2).

Together these findings support the utility of macrophage-targeted therapy for this disease. Despite this, there are significant differences in activity of G5-FA-MTX in this arthritis model and what was previously observed in tumor models. The 2 G5-FA-MTX lots used in this study were effective in suppressing arthritis, but the G5-FA-MTX-1 lot was ineffective as a tumoricidal agent (Baker JR Jr: unpublished observations). The 2 lots of G5-FA-MTX differed primarily in the average number of FA molecules conjugated to the surface of the G5 dendrimer (~2.5 in the first lot versus ~5 in the second). This suggested that polyvalent interactions that occur with FRβ may require less folate for targeting, or may be augmented by MTX interactions with this receptor to yield a sufficiently high binding affinity to obtain targeting. Further dose-ranging studies will clarify these effects. Unfortunately, the only previous study using a folate-conjugated G4 PAMAM to treat arthritis does not clarify these issues, because the drug involved (indomethacin) was complexed but not covalently linked to amine-surfaced dendrimers (33). Thus, the observed increase in indomethacin in the joint may be attributed

to nonspecific internalization of the positively charged dendrimer (47). Further confirmation of overall pharmacokinetics of folate targeting could come from magnetic resonance imaging of animals given folate and gadolinium–conjugated dendrimers (48).

In conclusion, we have demonstrated that FRβ-specific targeting of MTX into macrophages via dendrimers beneficially suppresses inflammatory changes associated with type II collagen–induced arthritis in rats. This approach may also serve as a useful targeted therapeutic strategy for treating other macrophage inflammatory diseases such as inflammatory bowel disease, granulomatous diseases, and atherosclerosis. Alternatively, the current FA-based dendrimer could be used as a platform to improve the delivery of other DMARDs such as the TNF blockers, gold salts, chloroquine (42,49), or NF-κB inhibitors (50).

ACKNOWLEDGMENTS

AUTHOR CONTRIBUTIONS

All authors were involved in drafting the article or revising it critically for important intellectual content, and all authors approved the final version to be published. Dr. Baker had full access to all of the data in the study and takes responsibility for the integrity of the data and the accuracy of the data analysis.
Study conception and design. Majoros, Cao, Baker.
Acquisition of data. Thomas, Goonewardena, Kotlyar, Cao, Baker.
Analysis and interpretation of data. Thomas, Goonewardena, Cao, Leroueil, Baker.

REFERENCES

1. Antony AC. Folate receptors. Annu Rev Nutr 1996;16:501–21.
2. Spiegelstein O, Eudy JD, Finnell RH. Identification of two putative novel folate receptor genes in humans and mouse. Gene 2000;258:117–25.
3. Low PS, Henne WA, Doorneweerd DD. Discovery and development of folic-acid-based receptor targeting for imaging and therapy of cancer and inflammatory diseases. Acc Chem Res 2008;41:120–9.
4. Cutolo M, Sulli A, Pizzorni C, Seriolo B, Straub RH. Anti-inflammatory mechanisms of methotrexate in rheumatoid arthritis. Ann Rheum Dis 2001;60:729–35.
5. Nakashima-Matsushita N, Homma T, Yu S, Matsuda T, Sunahara N, Nakamura T, et al. Selective expression of folate receptor β and its possible role in methotrexate transport in synovial macrophages from patients with rheumatoid arthritis. Arthritis Rheum 1999;42:1609–16.
6. Nagayoshi R, Nagai T, Matsushita K, Sato K, Sunahara N, Matsuda T, et al. Effectiveness of anti–folate receptor β antibody conjugated with truncated Pseudomonas exotoxin in the targeting of rheumatoid arthritis synovial macrophages. Arthritis Rheum 2005;52:2666–75.
7. Paulos CM, Turk MJ, Breur GJ, Low PS. Folate receptor-mediated targeting of therapeutic and imaging agents to activated macrophages in rheumatoid arthritis. Adv Drug Deliv Rev 2004;56:1205–17.
8. Paulos CM, Varghese B, Widmer WR, Breur GJ, Vlashi E, Low PS. Folate-targeted immunotherapy effectively treats established adjuvant and collagen-induced arthritis. Arthritis Res Ther 2006;8:R77.
9. Van der Heijden JW, Oerlemans R, Dijkmans BA, Qi H, van der Laken CJ, Lems WF, et al. Folate receptor β as a potential delivery route for novel folate antagonists to macrophages in the synovial tissue of rheumatoid arthritis patients. Arthritis Rheum 2009;60:12–21.
10. Xia W, Hilgenbrink AR, Matteson EL, Lockwood MB, Cheng JX, Low PS. A functional folate receptor is induced during macrophage activation and can be used to target drugs to activated macrophages. Blood 2009;113:438–46.
11. Turk MJ, Breur GJ, Widmer WR, Paulos CM, Xu LC, Grote LA, et al. Folate-targeted imaging of activated macrophages in rats with adjuvant-induced arthritis. Arthritis Rheum 2002;46:1947–55.
12. Hilgenbrink AR, Low PS. Folate receptor-mediated drug targeting: from therapeutics to diagnostics. J Pharm Sci 2005;94:2135–46.
13. Fiehn C. The future of folic acid antagonist therapy in rheumatoid arthritis [editorial]. Arthritis Rheum 2009;60:1–4.
14. Pincus T, Ferraccioli G, Sokka T, Larsen A, Rau R, Kushner I, et al. Evidence from clinical trials and long-term observational studies that disease-modifying anti-rheumatic drugs slow radiographic progression in rheumatoid arthritis: updating a 1983 review. Rheumatology (Oxford) 2002;41:1346–56.
15. Wessels JA, Huizinga TW, Guchelaar HJ. Recent insights in the pharmacological actions of methotrexate in the treatment of rheumatoid arthritis. Rheumatology (Oxford) 2008;47:249–55.
16. Cronstein BN. Low-dose methotrexate: a mainstay in the treatment of rheumatoid arthritis. Pharmacol Rev 2005;57:163–72.
17. Hu SK, Mitcho YL, Oronsky AL, Kerwar SS. Studies on the effect of methotrexate on macrophage function. J Rheumatol 1988;15:206–9.
18. Johnson WJ, DiMartino MJ, Meunier PC, Muirhead KA, Hanna N. Methotrexate inhibits macrophage activation as well as vascular and cellular inflammatory events in rat adjuvant induced arthritis. J Rheumatol 1988;15:745–9.
19. Puig-Kroger A, Sierra-Filardi E, Dominguez-Soto A, Samaniego R, Corcuera MT, Gomez-Aguado F, et al. Folate receptor β is expressed by tumor-associated macrophages and constitutes a marker for M2 anti-inflammatory/regulatory macrophages. Cancer Res 2009;69:9395–403.
20. Aletaha D, Smolen JS. The rheumatoid arthritis patient in the clinic: comparing more than 1,300 consecutive DMARD courses. Rheumatology (Oxford) 2002;41:1367–74.
21. Maetzel A, Wong A, Strand V, Tugwell P, Wells G, Bombardier C. Meta-analysis of treatment termination rates among rheumatoid arthritis patients receiving disease-modifying anti-rheumatic drugs. Rheumatology (Oxford) 2000;39:975–81.
22. Bohanec Grabar P, Logar D, Lestan B, Dolzan V. Genetic determinants of methotrexate toxicity in rheumatoid arthritis patients: a study of polymorphisms affecting methotrexate transport and folate metabolism. Eur J Clin Pharmacol 2008;64:1057–68.
23. Vicent MJ, Duncan R. Polymer conjugates: nanosized medicines for treating cancer. Trends Biotechnol 2006;24:39–47.
24. Thomas TP, Shukla R, Majoros IJ, Myc A, Baker JR Jr. Poly (amidoamine) dendrimer-based multifunctional nanoparticles. In: Mirkin CA, Niemeyer CM, editors. Nanobiotechnology II. More concepts and applications. Weinheim (Germany): Wiley-VCH Verlag GmbH & Co. KGaA; 2007. p. 305–19.

25. Svenson S, Tomalia DA. Dendrimers in biomedical applications—reflections on the field. Adv Drug Deliv Rev 2005;57:2106–29.

26. Nanjwade BK, Bechra HM, Derkar GK, Manvi FV, Nanjwade VK. Dendrimers: emerging polymers for drug-delivery systems. Eur J Pharm Sci 2009;38:185–96.

27. Konda SD, Aref M, Wang S, Brechbiel M, Wiener EC. Specific targeting of folate-dendrimer MRI contrast agents to the high affinity folate receptor expressed in ovarian tumor xenografts. MAGMA 2001;12:104–13.

28. Thomas TP, Majoros IJ, Kotlyar A, Kukowska-Latallo JF, Bielinska A, Myc A, et al. Targeting and inhibition of cell growth by an engineered dendritic nanodevice. J Med Chem 2005;48:3729–35.

29. Shukla R, Thomas TP, Peters J, Kotlyar A, Myc A, Baker JR Jr. Tumor angiogenic vasculature targeting with PAMAM dendrimer-RGD conjugates. Chem Commun (Camb) 2005;46:5739–41.

30. Shukla R, Thomas TP, Peters JL, Desai AM, Kukowska-Latallo J, Patri AK, et al. HER2 specific tumor targeting with dendrimer conjugated anti-HER2 mAb. Bioconjug Chem 2006;17:1109–15.

31. Kukowska-Latallo JF, Candido KA, Cao Z, Nigavekar SS, Majoros IJ, Thomas TP, et al. Nanoparticle targeting of anticancer drug improves therapeutic response in animal model of human epithelial cancer. Cancer Res 2005;65:5317–24.

32. Myc A, Majoros IJ, Thomas TP, Barker JR Jr. Dendrimer-based targeted delivery of an apoptotic sensor in cancer cells. Biomacromolecules 2007;8:13–8.

33. Chandrasekar D, Sistla R, Ahmad FJ, Khar RK, Diwan PV. The development of folate-PAMAM dendrimer conjugates for targeted delivery of anti-arthritic drugs and their pharmacokinetics and biodistribution in arthritic rats. Biomaterials 2007;28:504–12.

34. Majoros IJ, Keszler B, Woehler S, Bull T, Baker JR Jr. Acetylation of poly(amidoamine) dendrimers. Macromolecules 2003;36:5526–9.

35. Zhang Y, Thomas TP, Desai A, Zong H, Leroueil PR, Majoros IJ, et al. Targeted dendrimeric anticancer prodrug: a methotrexate-folic acid-poly(amidoamine) conjugate and a novel, rapid, "one pot" synthetic approach. Bioconjug Chem 2010. E-pub ahead of print.

36. Thomas TP, Ye JY, Chang YC, Kotlyar A, Cao Z, Majoros IJ, et al. Investigation of tumor cell targeting of a dendrimer nanoparticle using a double-clad optical fiber probe. J Biomed Opt 2008;13:014024.

37. McCarron RM, Goroff DK, Luhr JE, Murphy MA, Herscowitz HB. Methods for the collection of peritoneal and alveolar macrophages. Methods Enzymol 1984;108:274–84.

38. Myc A, Douce TB, Ahuja N, Kotlyar A, Kukowska-Latallo J, Thomas TP, et al. Preclinical antitumor efficacy evaluation of dendrimer-based methotrexate conjugates. Anticancer Drugs 2008;19:143–9.

39. Kinne RW, Brauer R, Stuhlmuller B, Palombo-Kinne E, Burmester GR. Macrophages in rheumatoid arthritis. Arthritis Res 2000;2:189–202.

40. Yanni G, Whelan A, Feighery C, Bresnihan B. Synovial tissue macrophages and joint erosion in rheumatoid arthritis. Ann Rheum Dis 1994;53:39–44.

41. Kinne RW, Stuhlmuller B, Burmester GR. Cells of the synovium in rheumatoid arthritis: macrophages. Arthritis Res Ther 2007;9:224.

42. Hamilton JA, Tak PP. The dynamics of macrophage lineage populations in inflammatory and autoimmune diseases [review]. Arthritis Rheum 2009;60:1210–21.

43. Bookbinder SA, Espinoza LR, Fenske NA, Germain BF, Vasey FB. Methotrexate: its use in the rheumatic diseases. Clin Exp Rheumatol 1984;2:185–93.

44. Turk MJ, Waters DJ, Low PS. Folate-conjugated liposomes preferentially target macrophages associated with ovarian carcinoma. Cancer Lett 2004;213:165–72.

45. Jaffee BD, Kerr JS, Jones EA, Giannaras JV, McGowan M, Ackerman NR. The effect of immunomodulating drugs on adjuvant-induced arthritis in Lewis rats. Agents Actions 1989;27:344–6.

46. Morgan SL, Baggott JE, Bernreuter WK, Gay RE, Arani R, Alarcon GS. MTX affects inflammation and tissue destruction differently in the rat AA model. J Rheumatol 2001;28:1476–81.

47. Thomas TP, Majoros I, Kotlyar A, Mullen D, Holl MM, Baker JR Jr. Cationic poly(amidoamine) dendrimer induces lysosomal apoptotic pathway at therapeutically relevant concentrations. Biomacromolecules 2009;10:3207–14.

48. Swanson SD, Kukowska-Latallo JF, Patri AK, Chen C, Ge S, Cao Z, et al. Targeted gadolinium-loaded dendrimer nanoparticles for tumor-specific magnetic resonance contrast enhancement. Int J Nanomedicine 2008;3:201–10.

49. Sokka T, Envalds M, Pincus T. Treatment of rheumatoid arthritis: a global perspective on the use of antirheumatic drugs. Mod Rheumatol 2008;18:228–39.

50. Hattori Y, Sakaguchi M, Maitani Y. Folate-linked lipid-based nanoparticles deliver a NFκB decoy into activated murine macrophage-like RAW264.7 cells. Biol Pharm Bull 2006;29:1516–20.